


Nanoscale structural evaluation of 0-3 magnetic nanocomposites fabricated by electro-infiltration

Cite as: AIP Advances **9**, 125028 (2020); <https://doi.org/10.1063/1.5130420@adv.2020.MMM2020.issue-1>

Submitted: 07 October 2019 . Accepted: 16 October 2019 . Published Online: 19 December 2019

Connor S. Smith, Sara C. Mills, Shehaab Savliwala, Carlos Rinaldi, Jennifer Andrew, and David P. Arnold 

COLLECTIONS

Paper published as part of the special topic on [64th Annual Conference on Magnetism and Magnetic Materials, Chemical Physics, Collection, Energy, Fluids and Plasmas, Materials Science and Mathematical Physics](#)

Note: This paper was presented at the 64th Annual Conference on Magnetism and Magnetic Materials.



View Online



Export Citation



CrossMark

ARTICLES YOU MAY BE INTERESTED IN

[Electrophoretic deposition of iron oxide nanoparticles to achieve thick nickel/iron oxide magnetic nanocomposite films](#)

AIP Advances **10**, 015308 (2020); <https://doi.org/10.1063/1.5129797>

[A 30-nm thick integrated hafnium zirconium oxide nano-electro-mechanical membrane resonator](#)

Applied Physics Letters **116**, 043501 (2020); <https://doi.org/10.1063/1.5134856>



NEW: TOPIC ALERTS

Explore the latest discoveries in your field of research

SIGN UP TODAY!

Nanoscale structural evaluation of 0-3 magnetic nanocomposites fabricated by electro-infiltration

Cite as: AIP Advances 9, 125028 (2019); doi: 10.1063/1.5130420

Presented: 6 November 2019 • Submitted: 7 October 2019 •

Accepted: 16 October 2019 • Published Online: 19 December 2019



Connor S. Smith,^{1,a)} Sara C. Mills,² Shehaab Savliwala,³ Carlos Rinaldi,^{3,4} Jennifer Andrew,² and David P. Arnold¹ 

AFFILIATIONS

¹Department of Electrical and Computer Engineering, Gainesville, Florida 32611, USA

²Department of Materials Science and Engineering, Gainesville, Florida 32611, USA

³Department of Chemical Engineering, Gainesville, Florida 32611, USA

⁴J. Crayton Pruitt Family Department of Biomedical Engineering, Gainesville, Florida 32611, USA

Note: This paper was presented at the 64th Annual Conference on Magnetism and Magnetic Materials.

a)Corresponding author. Tel.: +1-440-315-7896. E-mail address: connor.smith@ufl.edu

ABSTRACT

Magnetic nanocomposites with 0-3 connectivity, whereby a 0D magnetic nanoparticle phase is embedded into a 3D magnetic metal matrix phase, have gained increased interest for use in applications ranging from integrated power inductor cores to exchange-spring magnets. The electro-infiltration process, in which a metal phase is electroplated through a nanoparticle film phase, is an inexpensive approach compatible with semiconductor fabrication methods for the formation of these nanocomposites. Past demonstrations of electro-infiltrated nanocomposites have relied on scanning electron microscopy and energy dispersive x-ray spectroscopy to evaluate the 0-3 composite structure. However, a detailed investigation of the boundary between the particle and metal matrix phases cannot be performed with these tools, and it is unknown whether the particle/matrix interfaces are dense and void-free. This detail is critical, as the presence of even nanoscale voids would affect any potential magnetic exchange coupling and hence the overall electromagnetic properties of the material. This work seeks to explore the phase boundary of 0-3 magnetic nanocomposite fabricated by electro-infiltration by using scanning transmission electron microscopy and energy-dispersive x-ray spectroscopy to analyze the nanostructure of two different composites—a nickel/iron-oxide composite and a permalloy/iron-oxide composite. High-resolution imaging indicates that the interface between the particle phase and matrix phase is dense and void-free. These results will help guide future studies on the design and implementation of these magnetic nanocomposites for end applications.

© 2019 Author(s). All article content, except where otherwise noted, is licensed under a Creative Commons Attribution (CC BY) license (<http://creativecommons.org/licenses/by/4.0/>). <https://doi.org/10.1063/1.5130420>

I. INTRODUCTION

The fabrication and application of magnetic nanocomposites, defined by having one or more of their phases possess a characteristic length scale of 1-100 nm, has gained interest due to the desire for new and better hard and soft magnetic materials. These new materials could decrease reliance on rare-earth magnets and improve the performance and efficiency of devices in areas such as power electronics (Sullivan, 2009; Balamurugan *et al.*, 2012; Coey, 2012; Lewis and Jimenez-Villacorta, 2013; Sullivan *et al.*, 2013; and Silveyra *et al.*, 2018). Figure 1a shows the structure of a 0-3 magnetic nanocomposite, which is made from magnetic nanoparticles surrounded by a

magnetic metal matrix. These composites have been made using different methods, such as cluster deposition, which requires the use of expensive and/or modified equipment (Balasubramanian *et al.*, 2011 and Liu *et al.*, 2011), and magnetic composite electroplating, which results in low fill ratios on the order of <5% (Guan and Nelson, 2005; 2006). Over the last decade the electro-infiltration method, developed by Hayashi *et al.* and Wen *et al.*, has been suggested as a relatively cheap and semiconductor fabrication compatible method for making 0-3 magnetic particle/matrix composites (Hayashi *et al.*, 2012; Wen *et al.*, 2014; 2016; 2017; and Smith *et al.*, 2019).

The magnetic and material properties of 0-3 electro-infiltrated composites have been previously documented for various

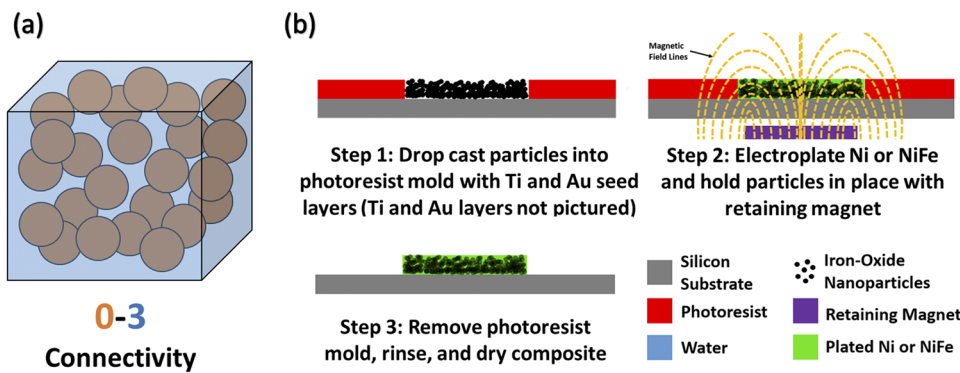


FIG. 1. (a) Example of the structure of a composite material with 0-3 connectivity. (b) Electroinfiltration process used to fabricate Ni/ION and NiFe/ION samples in this study. Photoresist is patterned on a silicon substrate, and iron-oxide nanoparticles were drop cast into the molds. Ni or NiFe is electroplated through the porous particle film while the particles are held in place with a retaining magnet, forming a composite material.

applications (Wen *et al.*, 2016; 2017; and Smith *et al.*, 2019). These works relied on scanning electron microscopy (SEM) and energy dispersive x-ray spectroscopy (EDS) to demonstrate successful electro-infiltration, but these methods do not afford the spatial resolution to analyze the boundary between the particle and matrix phases. The phase boundary of these composites is of great importance, because the presence of voids between the particles and the metal matrix can significantly affect the properties of the material as a whole. Specifically, voids between the particle and matrix phases is of known importance for applications such as exchange-spring magnets, where voids would negatively effect the exchange-coupling interactions of the two phases (Skomski and Coey, 1993). The phase boundary is also of importance in inductor core materials, where voids would degrade the overall permeability of the core (Silveyra *et al.*, 2018).

This work explores the phase boundary between the particles and metal matrix of 0-3 nanocomposites made using electroinfiltration. To do this, high-resolution S/TEM combined with EDS, is used to probe two different composite samples—a nickel/iron-oxide composite and a permalloy/iron-oxide composite. Results show that the iron-oxide nanoparticles (IONs) are surrounded by metal to form a dense, void-free boundary.

II. MATERIALS AND METHODS

Iron-oxide nanoparticles with an average diameter of 31 nm were synthesized using a two-step semi-batch thermal decomposition method adapted from Vreeland *et al.* and put into suspension (Vreeland *et al.*, 2015). The electroinfiltration process flow can be seen in Fig. 1b. First, a photoresist layer is patterned on top of a silicon substrate that has a 20 nm titanium (Ti) adhesion layer and a 100 nm gold (Au) seed layer sputtered upon it, and the iron-oxide nanoparticles are drop cast into the resulting molds. These molds are left to dry into a porous particle film for at least 3 hours in a fume hood. In the next step, the particle layer is placed into an electroplating bath of either Ni or NiFe, where these metals are electroplated through the film at a current density of 10 mA/cm² at 54°C (for Ni) or 25°C (for NiFe) with no agitation. A NdFeB retaining magnet, placed ~1 cm from the backside of the substrate, is used to hold the magnetic particles in place during plating. Finally, the film is removed from the plating bath, rinsed, and the photoresist layer is stripped to leave behind a composite material. After

fabrication, a FEI Helios NanoLab 600 Dual-Beam FIB/SEM was used to cut lamellae of the composite materials, and S/TEM images were taken using a FEI Tecnai F20 S/TEM instrument operating at 200 keV with an EDS detector.

III. RESULTS AND DISCUSSION

A. Identification of layers within the sample cross-sections

EDS line scans taken along the thickness of each of the samples are used to reveal and identify the presence different layers formed during fabrication. Fig. 2a shows a line scan plot for the Ni/ION composite with each layer labeled, and Fig. 2b shows a line scan plot for the NiFe/ION composite with each layer labeled. In Fig. 2a, the presence of silicon and silicon oxide come from the substrate. Following these should be a 20 nm titanium adhesion layer, but this does not appear due to the low resolution of the line scan. Instead, the 100 nm gold seed layer is observed, present directly above the substrate. After this, the 2 μ m Ni/ION composite layer appears, as supported by the combined presence of nickel and iron in the line scan. After the composite layer, a transition is made to a pure nickel layer. Due to the presence of an un-infiltrated layer of particles that is ~1 μ m thick above the pure nickel layer, it is suggested that stress from the electroplating step caused the nickel to stop infiltrating the particle layer and, instead, heave it upward as pure nickel continued to plate below it. The exact cause of this phenomenon requires further exploration.

In Fig. 2b, after the expected silicon, silicon oxide, and gold layers, the NiFe/ION composite layer comes into view. Unlike the Ni/ION composite, this layer does not transition into a pure NiFe layer at any point, and instead transitions to an un-infiltrated particle layer. This transition suggests the plating step had been stopped prematurely before the particle layer could be filled, or before stress caused the particle layer to be heaved up, as seen in Fig. 2a.

B. Inspection of composite layers via S/TEM

Next, inspection of the different layers of the cross-section is necessary to examine how the particles are distributed throughout the material and better understand the connectivity of the composite. Fig. 3 shows S/TEM images taken of the Ni/ION and NiFe/ION composite samples. In Fig. 3a, we can see the Ni/ION composite

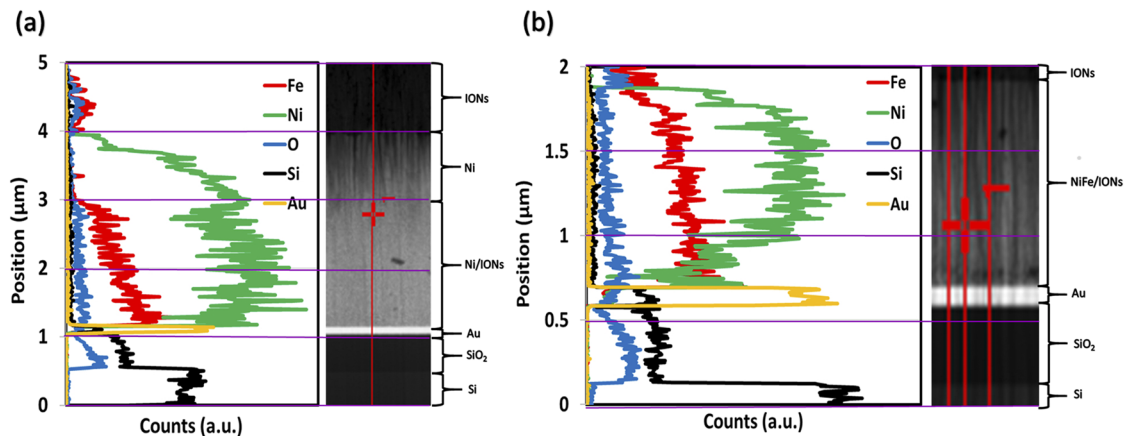


FIG. 2. (a) Labeled EDS line scan of the cross-section of the Ni/ION composite and (b) labeled EDS line scan of the cross-section of the NiFe/ION composite. The specific layers present throughout the sample are noted in the image, including the added layer used during FIB sample preparation. Layers are identified by the elements seen within them.

layer, which appears to be densely filled with nanoparticles. The presence of different shades of black and gray from one nanoparticle to the next seen in this image is a consequence of the lack of alignment of the different particles and their crystal orientations. In Fig. 3b, an image of the pure nickel layer can be seen, with a lack of the many nanoparticles that were densely packed in the Ni/ION layer. A few single IONs can be seen within this layer, but the make-up is primarily nickel metal. In Fig. 3c, the un-infiltrated layer of particles can be seen, with the various un-infiltrated nanoparticles visible and surrounded by empty space. Due to Z-contrast, elements with greater atomic mass are shown to be brighter.

The presence of nanoparticles in the pure nickel layer, as seen in Fig. 3b, was previously unknown, and supports the idea that the

pure nickel layer heaves up the un-infiltrated particle layer after some point during the plating step, as the particles seen in the pure nickel layer may have fell off during this lifting process and were surrounded by nickel.

Fig. 3d shows the cross-section of the NiFe/ION composite layer, with nanoparticles present throughout. Fig. 3e shows the interface between the NiFe/ION composite layer and the un-infiltrated particles layer, which indicates the position where the electroplating of the permalloy was stopped. Finally, in Fig. 3f, the un-infiltrated nanoparticle layer in the sample is shown, with particles shown to be densely packed together and surrounded by empty space. These images support that there has been a successful infiltration of permalloy through the particle layer, as particles embedded in the metal matrix are clearly visible.

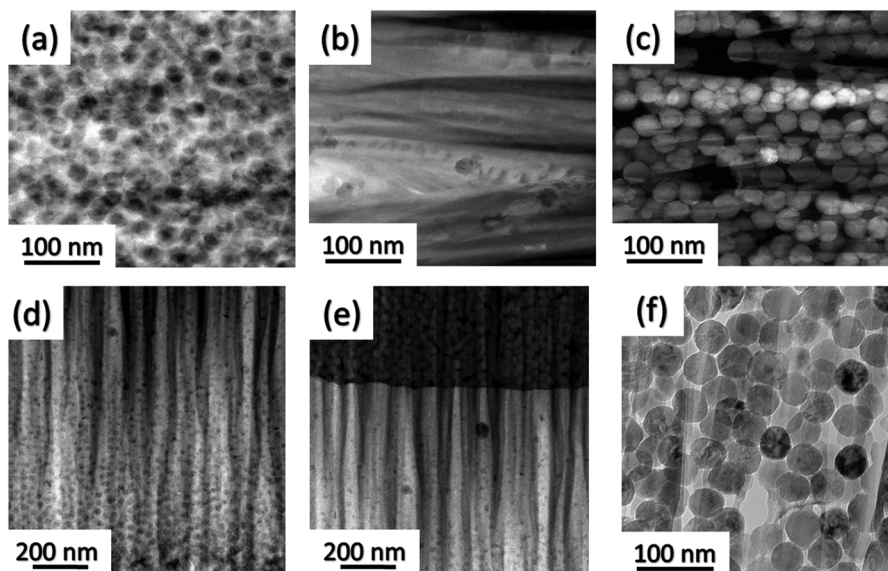


FIG. 3. S/TEM images of the Ni/ION and NiFe/ION composite samples. Images (a-c) correspond to the Ni/ION sample, showing (a) a close-up view of the composite layer, (b) the pure nickel layer, and (c) the excess ION layer. Note the presence of a few errant particles in the pure nickel layer. Images (d-f) correspond to the NiFe/ION sample, showing (a) a close-up view of the composite layer, (b) the interface between the composite layer and the excess ION layer, and (c) the excess ION layer.

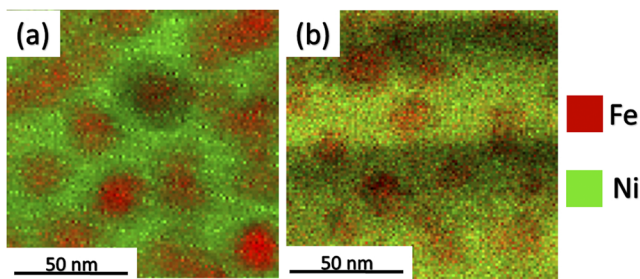


FIG. 4. EDS mapping of (a) the Ni/ION composite sample and (b) the NiFe/ION composite sample, indicating the presence of iron in red, and the presence of nickel in green. Note the clear separation between the iron signal (coming from the nanoparticles) and the nickel signal (coming from the matrix) in (a), while such a separation is still present, but less visible in (b) due the presence of iron in both the particles and in the matrix (Ni-Fe). These images also indicate that the nanoparticles are completely surrounded by the metal matrix, with no visible voids surrounding them.

C. EDS confirmation of particle/matrix interface and composition

The final part of this investigation confirms that the electroplated metals do surround the particles in the composite and form a dense and void-free boundary, as evaluated with 2D EDS mapping. Fig. 4 shows two high-resolution EDS maps of an area in each of the two composites, with Fig. 4a showing the Ni/ION composite, and Fig. 4b showing the NiFe/ION composite. The color green represents the presence of nickel, and the color red represents the presence of iron. In Fig. 4a, there is a clear separation between the nickel matrix (green) and the iron-oxide nanoparticles (red) without any visible voids, indicating a dense, void-free boundary between the two phases. Likewise, Fig. 4b shows a similar behavior for the NiFe/ION composite layer, where the Ni-Fe matrix (red and green) are separate from the iron-oxide nanoparticles (red), with no visible voids present at their interfaces. These images support the conclusion that these composite materials successfully lead to a lack of voids between the particle and matrix phases.

IV. CONCLUSION

This work offers a definite confirmation that the boundary between the particle and metal matrix phase of electro-infiltrated Ni/ION and NiFe/ION nanocomposites are dense, and void-free. Previous studies of these composites confirmed the successful infiltration by examining the properties of the composites and/or through the use of SEM and EDS, but investigation of the phase boundary was limited by resolution. Through the use of S/TEM and EDS, it is now known that metals electroplated through particle film in the electro-infiltration process do fill in the spaces between particles which leads to a dense and void-free boundary. This dense, void-free interface between the particle and matrix phases in the composites is necessary for applications such as exchange-spring magnets and improved inductor cores, and further suggests the electro-infiltration fabrication process as an attractive pathway towards realizing such materials. This work provides support for past studies on electro-infiltrated 0-3 nanocomposites and

encourages further investigations on the applications of these composite materials.

ACKNOWLEDGMENTS

This work was funded in part by the National Science Foundation (CMMI-1727930). The authors thank the staff of the Herbert Wertheim College of Engineering Research Service Center at the University of Florida for assistance in the fabrication and material analysis.

REFERENCES

- Balamurugan, B., Sellmyer, D. J., Hadjipanayis, G. C., and Skomski, R., "Prospects for nanoparticle-based permanent magnets," *Scr. Mater.* **67**, 542–547 (2012).
- Balasubramanian, B., Skomski, R., Li, X., Valloppilly, S. R., Shield, J. E., Hadjipanayis, G. C., and Sellmyer, D. J., "Cluster synthesis and direct ordering of rare-earth transition-metal nanomagnets," *Nano Lett.* **11**(4), 1747–1752 (2011).
- Coey, J. M. D., "Permanent magnet: Plugging the void," *Scr. Mater.* **67**, 524–529 (2012).
- Guan, S. and Nelson, B. J., "Pulse-reverse electrodeposited nanograined CoNiP thin films and microarrays for MEMS actuators," *J. Electrochem. Soc.* **152**(4), C190 (2005).
- Guan, S. and Nelson, B. J., "Magnetic composite electroplating for depositing micromagnets," *J. Microelectromechanical Syst.* **15**(2), 330–337 (2006).
- Hayashi, Y., Hashi, S., and Ishiyama, K., "Magnetic properties of nanostructured film composed of Co-ferrite nanoparticles and metal Co prepared by combination of electrophoretic deposition and electroplating," *IEEE Trans. Magn.* **48**(11), 3170–3173 (2012).
- Lewis, L. H. and Jimenez-Villacorta, F., "Perspectives on permanent magnetic materials for energy conversion and power generation," *Metall. Mater. Trans. A* **44**, S2–S20 (2013).
- Liu, X., He, S., Qiu, J. M., and Wang, J. P., "Nanocomposite exchange-spring magnet synthesized by gas phase method: From isotropic to anisotropic," *Appl. Phys. Lett.* **98**(22), 96–99 (2011).
- Silveyra, J. M., Ferrara, E., Huber, D. L., and Monson, T. C., "Soft magnetic materials for a sustainable and electrified world," *Science* **362**(418), 1–9 (2018).
- Skomski, R. and Coey, J. M. D., "Giant energy product in nanostructured two-phase magnets," *Phys. Rev. B* **48**(21), 812–816 (1993).
- Smith, C. S., Savliwala, S., Mills, S. C., Andrew, J. S., Rinaldi, C., and Arnold, D. P., "Electro-infiltrated nickel/iron-oxide and permalloy/iron-oxide nanocomposites for integrated power inductors," *IEEE J. Magn. Mater.* **493**, 165718 (2019).
- Sullivan, C. R., "Integrating magnetism for on-chip power: Challenges and opportunities," *Proc. Cust. Integr. Circuits Conf.*, no. Cicc (2009), pp. 291–298.
- Sullivan, C. R., Harburg, D. V., Qiu, J., Levey, C. G., and Yao, D., "Integrating magnetism for on-chip power: A perspective," *IEEE Trans. Power Electron.* **28**(9), 4342–4353 (2013).
- Vreeland, E. C., Watt, J., Schober, G. B., Hance, B. G., Austin, M. J., Price, A. D., Fellows, B. D., Monson, T. C., Hudak, N. S., Maldonado-Camargo, L., Bohorquez, A. C., Rinaldi, C., and Huber, D. L., "Enhanced nanoparticle size control by extending LaMer's mechanism," *Chem. Mater.* **27**(17), 6059–6066 (2015).
- Wen, X., Andrew, J. S., and Arnold, D. P., "Exchange-coupled hard magnetic Fe-Co/CoPt nanocomposite films fabricated by electro-infiltration," *AIP Adv.* **7**(5), 056225 (2017).
- Wen, X., Kelly, S. J., Andrew, J. S., and Arnold, D. P., "Nickel-zinc ferrite/permalloy ($\text{Ni}_{0.5}\text{Zn}_{0.5}\text{Fe}_2\text{O}_4/\text{Ni-Fe}$) soft magnetic nanocomposites fabricated by electro-infiltration," *AIP Adv.* **6**(5), 056111 (2016).
- Wen, X., Starr, J. D., Andrew, J. S., and Arnold, D. P., "Electro-infiltration: A method to form nanocomposite soft magnetic cores for integrated magnetic devices," *J. Micromechanics Microengineering* **24**(10), 107001 (2014).